Pyrometric temperature controller for million degree per second heating

S. Brauer, D. H. Ryan, J. O. Ström-Olsen, and M. Sutton
Department of Physics, McGill University, Rutherford Building, 3600 University Street, Montréal, Québec, H3A 2T8, Canada

G. B. Stephenson
IBM Research Division, T. J. Watson Research Center, Yorktown Heights, New York 10598

(Received 26 March 1990; accepted for publication 3 May 1990)

A high-power proportional temperature controller, using a fast infrared pyrometer, has been developed to change and control the temperature of metallic ribbon samples with microsecond response. The apparatus provides uniform and controlled heating for time-resolved x-ray scattering studies of structural phase transitions. When high-power pulse heating is used, the system is capable of increasing the sample temperature at rates in excess of 10^6 K/s, without overshoot and with subsequent control to $\pm$ 1 K at temperatures as low as 650 K.

I. INTRODUCTION

Time-resolved scattering has become a powerful experimental technique for investigating transitory phenomena in condensed matter systems.[1-4] Because of the very high intensity of synchrotron light sources and developments in high flux optics and fast detector systems, it is now possible to acquire detailed structural information with millisecond time resolution,[5] orders of magnitude faster than was possible only a few years ago. These advances have generated many new challenges for changing and controlling the state of the system under study on very short time scales.

Our time-resolved x-ray scattering experiments have concentrated on the kinetics of structural phase transitions in metallic systems. In these experiments, phase transformation is brought about by abruptly heating or cooling a specimen to a temperature where the structure is not stable. X-ray diffraction patterns are repeatedly acquired as the system evolves toward thermodynamic equilibrium at the new temperature. This work is carried out at the National Synchrotron Light Source on the IBM/MIT beamline, X-20C. With an incident flux of 10^{13} photons per second and a fast linear position sensitive detector, powder diffraction patterns can be acquired as quickly as every 3 ms.

For such studies to be deemed isothermal (which is important in any quantitative analysis of the results), the transient of the temperature step must be much shorter than the phase transformation time. To take full advantage of the available time resolution, it is necessary to develop techniques to change sample temperature, in a uniform and controlled manner, by hundreds of degrees in milliseconds.

In a recent article,[6] we described a thermal geometry that permits controlled quenching of ribbon samples at rates in excess of 10^3 K/s. Here, we discuss improvements in temperature control for studying phase transitions that require a step *increase* of temperature, such as the crystallization of amorphous metals. The temperature controller uses a simple, inexpensive, yet fast infrared pyrometer and a high-power pulse heating technique to heat samples uniformly at rates in excess of 10^6 K/s with subsequent nonovershooting control to $\pm$ 1 K. Heating rates are comparable to the cooling rates achieved during the melt spinning of metallic glasses so that the system can be used to investigate the kinetics of crystallization in amorphous metals near the glass transition.

II. SAMPLES AND THERMAL GEOMETRY

Temperature control on fast time scales requires high heating and cooling power, and samples of small heat capacity. The characteristic time to achieve thermal equilibrium is then short, so that the temperature can be abruptly changed, and thermal disturbances such as variations in sample properties can be quickly and efficiently compensated.

Melt-spun ribbon segments, typically 35 mm long, 1 mm wide, and 25 μm thick, are well suited for our studies since they provide a small thermal mass yet appreciable surface area for x-ray scattering. When suspended between water cooled posts in helium gas, these samples can be heated resistively to temperatures in the range 500–1100 K by passing direct current along their length. In steady state, Joule heat generated throughout the volume of the sample is removed from the surface by radiation and heat exchange with the gas. Full advantage is taken of the small thermal mass as only the sample and a small volume of surrounding gas are heated. Furthermore, the heating power is limited only by the maximum available current. High cooling power is obtained, with little effect on the x-ray scattering, by filling the sample chamber with $\sim$30 kPa of helium. (Cooling is marginally improved if the pressure is increased beyond this value.) Since the heat capacity is proportional to sample volume, and the cooling power is proportional to surface area, the thermal time constant of a ribbon is inversely proportional to its thickness. This high-power, low-thermal load configuration gives a 200-ms thermal time constant for small temperature changes at 1000 K. For quenches of a few hundred degrees, cooling rates of more than 10^3 K/s are typical.

For thin ribbons of uniform cross section, the geometry produces a large central region of uniform temperature, because conduction along the ribbon and thermal gradients through the ribbon thickness are negligible. Measured and

 0034-6748/90/082214-06$02.00

calculated temperature distributions along one half of the length of an Fe_3B sample in the steady state are shown in Fig. 1. The temperature is constant within 1 K over the central 10 mm of the ribbon. This is ample in light of our 1×1 mm^2 x-ray beam spot. If the power to the sample was stepped from zero to a higher constant value, the temperature distribution (for a uniform, nontransforming specimen), would start out flat and grow to be higher and more rounded in approach to the equilibrium shape. However, as discussed in Sec. IV, we measure and control the temperature at the center of the ribbon and supply power to force the temperature there to step quickly up to the new set point. To do this, enough heat is deposited in the sample at the start to bring almost the whole length to the control temperature. The distribution then relaxes to the steady-state profile from above. Hence, the gradients in the final profile represent an upper limit of temperature nonuniformity.

III. FAST PYROMETER

In addition to a small thermal time constant, fast temperature control requires a temperature sensor with a frequency response greater than the bandwidth of control. Furthermore, only remote temperature measurement is practical in these studies since even very small contacting probes reduce thermal time response and perturb the temperature uniformity. To meet these demands, a focusing infrared pyrometer with microsecond response has been constructed. The device is ideal for low-signal, low-temperature pyrometry where fast response is required.

The photoconductive sensor is a chemically deposited polycrystalline layer of lead selenide, a narrow-band-gap semiconductor.[7] The device has an active area of 2×2 mm.^{2} Because the conductivity of PbSe is strongly dependent on temperature, and because its infrared sensitivity is increased roughly tenfold by cooling from 300 to 77 K, the device is anchored to the bottom of a custom built 0.2-ℓ liquid nitrogen Dewar (Fig. 2), which has a holding time of about 4 h. At 77 K the spectral response of PbSe is 1–7 μm, well suited for low-temperature pyrometry. The measured photoconductive time constant is 25 ± 2 μs. The fast response is largely due to the high number of grain surface acceptor states, which reduce the optical carrier recombination time.[8]

A pair of quartz lenses arranged with the sensor at one focus and the sample at the other collect roughly 500 times as much infrared radiation as without focusing. With this geometry, all pyrometer components are well removed from the x-ray scattering volume. Moreover, large lens separation is possible so that the Dewar can be positioned at a convenient distance from the goniometer mounted sample chamber. Because there is a $1.3\times$ reduction with the lenses shown, the detected spot has a full width at half maximum of 4 mm, as measured with a thin hot filament in vacuum.

The detector dark resistance at 77 K is $\sim$ 1 GΩ. To measure changes in this very large impedance, a low-noise, low-drift current preamplifier (see Fig. 3) is housed at room temperature within the Dewar vacuum space. This well-shielded arrangement reduces electronic pickup, and minimizes instability problems because the sensor is well shielded and close to the primary amplifier. Figure 4 shows the output voltage as a function of temperature for a 1-mm-wide ribbon. The solid curve is the (scaled) blackbody energy density formula evaluated at 2.2 μm, the effective pyrometer wavelength. The signal-to-noise ratio (S/N) is typically 100 when focused on a 1-mm-wide ribbon at 900 K, shot noise across the PbSe being the dominant noise source. The S/N

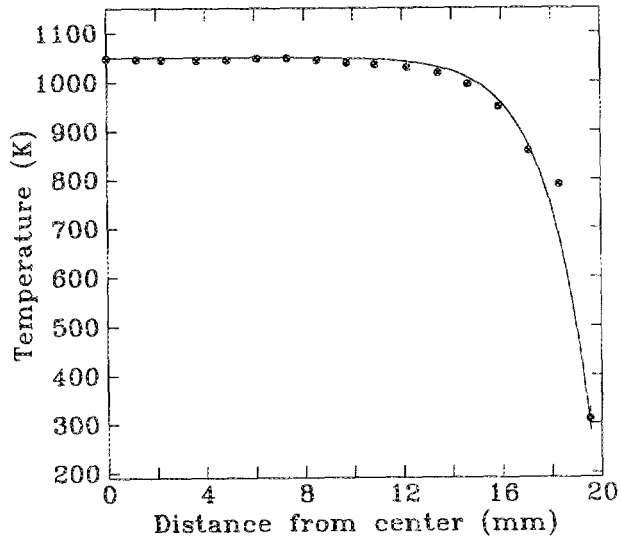

FIG. 1. Steady-state temperature distribution along one half of a Fe_3B ribbon sample. Measurements using the commercial pyrometer are shown as points. The solid curve is a one-dimensional finite difference solution to the heat equation with uniform power input per unit sample volume. Emissivity was assumed to be 0.1, thermal conductivity estimated to be 30 W K^{-1} m^{-1}, and the linear coefficient of convective heat transfer to the gas was adjusted to give the central temperature observed experimentally with the same input power. The temperature is constant within 1 K over the central 10 mm of the ribbon.

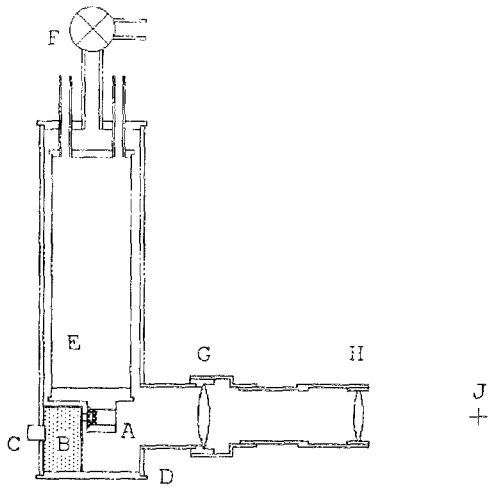

FIG. 2. Schematic of PbSe pyrometer. A: photoconductive sensor and 77-K radiation shield; B: room-temperature preamplifier; C: electrical feedthrough; D: InSn solder seal around removable base; E: liquid nitrogen can; F: vacuum-space valve; G: quartz lens ($f = 60$ mm) with epoxy vacuum seal; H: quartz lens ($f = 76$ mm) on telescopic mount; J: position of sample.

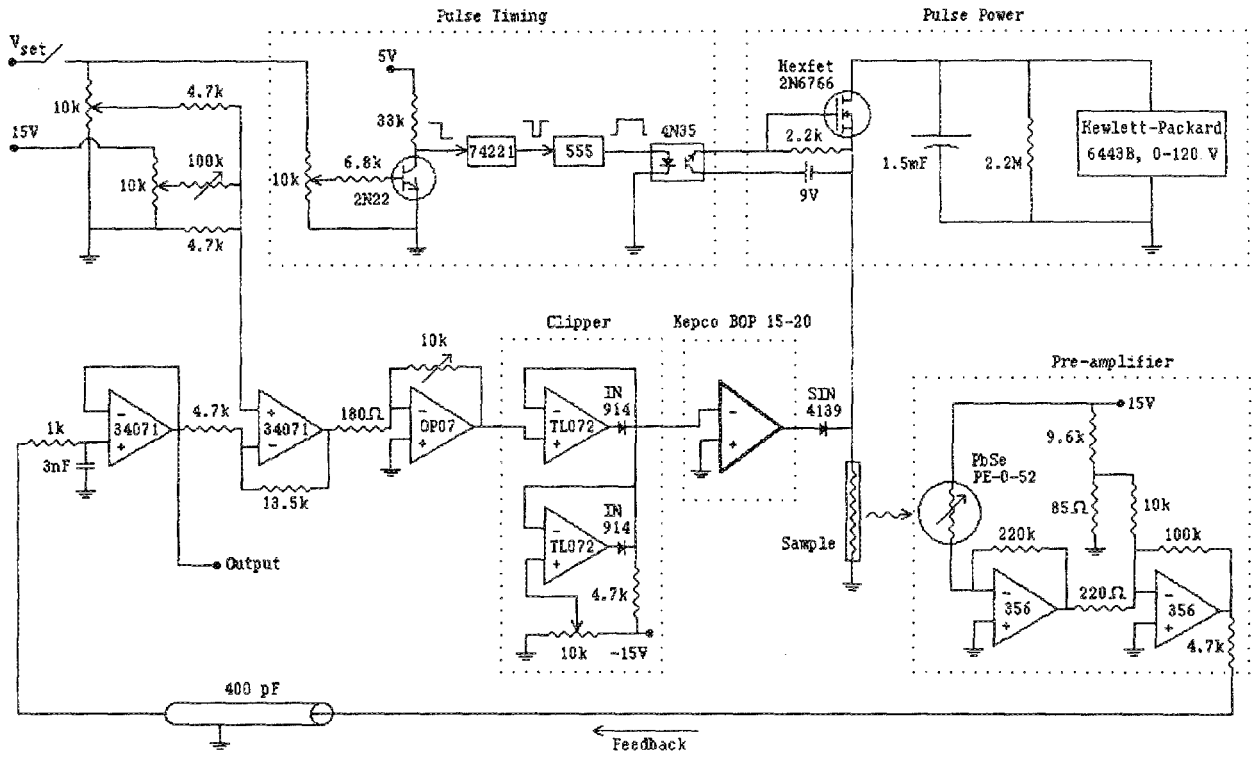

FIG. 3. Proportional temperature control circuit with pulse heating capability. Photoconductive changes in the PbSe detector are preamplified, passively filtered, and buffered to give the pyrometer output. The DAC controlled set-point voltage V_{set} is offset and divided to a convenient level before being compared to the pyrometer output at the second 34071 amplifier. The resulting error signal is amplified by a variable gain OP-07 and a power supply/amplifier (Kepco BOP 15-20) to regulate the voltage across the sample. Infrared radiation from the resistively heated specimen is collected and focused on the PbSe sensor, completing the feedback loop. The clipping circuit prevents the power amplifier from being driven to saturation in response to a step in set point. Orders of magnitude increase in heating rate are achieved when pulse heating is added to the control loop. A step in set point triggers a variable duration pulse that, through an optical coupler, turns on the Hexfet power transistor. The 1.5-mF capacitor bank, charged to ~120 V, discharges across the sample for the duration of the pulse, heating the specimen at over 10^6 K/s.

falls to 1 for ribbons at 600 K but with larger specimen emittance the pyrometer could be used to somewhat lower temperatures. Although simple quartz lenses provide sufficient transmittance for our work, replacement of the optical components with CaF_2 would improve S/N significantly.

A cold shroud around the detector masks its view of the outer vacuum can, which, because of the large solid angle it subtends at the sensor, would otherwise contribute an appreciable time varying background signal as the can temperature changed. Variations in lens temperature still appear, however, as a slowly varying pyrometer baseline that must be adjusted before each run. Although inconvenient, the effect is not important for our experiments, which usually last less than a few minutes.

Figure 5 shows the geometry in which we use the pyrometer. In the center of the ribbon, x-rays are scattered from the top surface while the temperature is read by two pyrometers from below (Fig. 5). The fast PbSe pyrometer output is used for feedback control, while the second pyrometer,[9] with 10-ms time constant, provides an independent measure of the steady-state temperature. Because sample emissivity and infrared attenuation are not precisely known, absolute calibration of $\pm$ 5 K can be achieved by using the known temperature dependence of the phase transformation being studied.

IV. TEMPERATURE CONTROL LOOP

To change and control temperature during crystallization studies of amorphous metal ribbons, the PbSe pyrome-

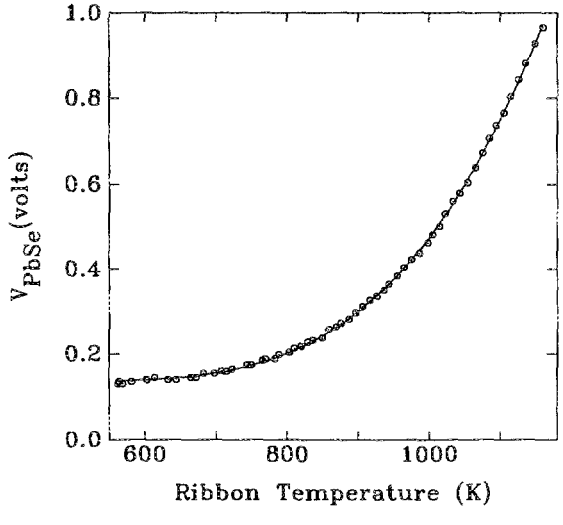

FIG. 4. Variation of PbSe pyrometer output voltage V with ribbon temperature. The solid curve is the scaled blackbody energy density evaluated at 2.2 μm, the effective pyrometer wavelength.

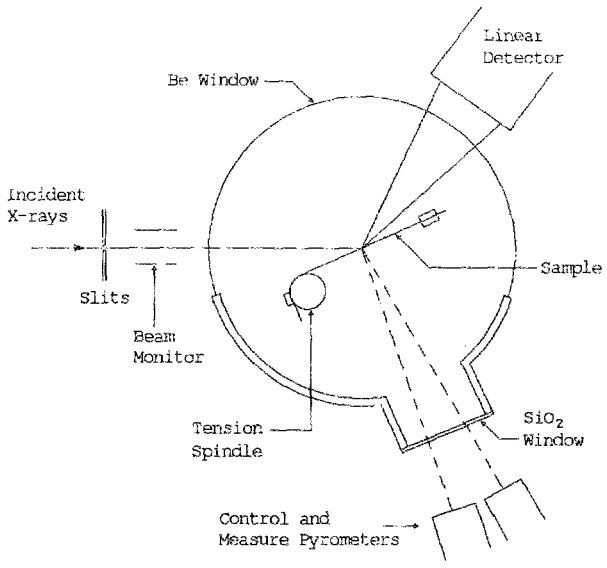

FIG. 5. Schematic of the experimental setup used in time-resolved x-ray scattering experiments.

ter is used in a feedback control loop. The controller is designed for rapidly increasing the sample temperature and then holding it constant in spite of sample resistance changes and the release of latent heat of crystallization. For these irreversible phase transitions it is crucial to avoid overshoot in a temperature step since the transformation kinetics vary exponentially with temperature.[10] For example, in $NiZr_2$ near 640 K, the time to crystallize 50 vol. % is halved with each 8 K increase in temperature.[1] Temperature overshoot would thus yield misleading results for transformation kinetics.

Details of the feedback system are shown in Fig. 3. The thermal time constant of the ribbon, $\tau_1 = 200$ ms, dominates all other time lags around the loop. As long as all other lags are small, the system time response is given by

$$\tau = \tau_1/(1+G), \tag{1}$$

where G is the open loop gain. Such a system does not overshoot in response to a step in set point, but rather relaxes exponentially to the new setting with characteristic time τ. As the gain is increased to improve step response, the system time constant will be reduced as given by (1) until it approaches the next largest system lag, τ_2. This is the 25-μs response of the PbSe pyrometer. The system is then a *quadratic lag* controller[11] as indicated schematically by Fig. 6, where $I(s)$ is the input set-point voltage and $O(s)$ is the pyrometer output. The Laplace transform of the closed loop gain gives the transfer function of the controller:

$$\frac{O(s)}{I(s)} = \frac{G}{(1+G)} \frac{\omega_n^2}{s^2 + 2\xi\omega_n s + \omega_n^2}, \tag{2}$$

where

$$\omega_n = \sqrt{(1+G)/\tau_1\tau_2}$$

is the natural response frequency and

$$\xi = \sqrt{(\tau_1+\tau_2)^2/4\tau_1\tau_2(1+G)}$$

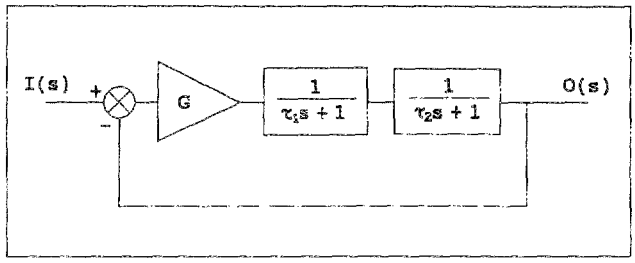

FIG. 6. Model of temperature control loop in the Laplace domain.

is the damping coefficient in the usual notation. Although such a system is intrinsically stable against self sustained oscillations for all G, it will overshoot in response to step input $[I(s) = 1/s]$, if the poles of Eq. (2) have a nonzero imaginary component. This occurs for $\xi < 1$.

For fastest nonovershooting step response, a *quadratic lag* control system should be operated at critical damping ($\xi = 1$), where the two poles of the transfer function to merge yield an ideal unit step response:

$$O(t) = \frac{G}{(1+G)}(1 - e^{-\omega_n t}). \tag{3}$$

In this ideal model of the controller, critical damping would be achieved with $G = 2000$, providing a system time constant of $\tau = 1/\omega_n = 50\ \mu$s. In practice, the control loop is not stable for an open loop gain of more than 1000, above which irregular temperature jumps are observed. Nonetheless, with $G = 1000$, a system time response of 75 μs is obtained and damping is subcritical with $\xi = 1.4$. Under these conditions, the steady-state error $(1+G)^{-1}$, is 0.1%. Excursions and recovery times from external disturbances are minimized by using this maximum permissible gain. If constant emissivity is assumed, temperature stability of ± 1 K is typical, even when the sample resistance changes by 25% during the experiment. For noise rejection, the feedback bandwidth is limited to 67 kHz by a passive filter, a factor of 30 above the system corner frequency.

It is common to attempt to improve control system performance by the addition of integral and/or differential dynamic compensation. Integral compensation reduces the steady-state error to zero. In our application, a constant steady-state error is inconsequential as it represents a small monotonic shift on our calibrated temperature scale. The only significant effect of integral control is to reduce time response. Derivative compensation on the other hand, has the effect of increasing the system damping and thus permitting a higher gain and faster response. However, with $\tau_1 \sim 1000\tau_2$, the system is intrinsically well damped so that simple proportional control gives excellent response.

Figure 7(a) shows the PbSe pyrometer output and the voltage across the sample for a typical temperature step with a crystallized Fe_3B ribbon. The proportional response is delayed by the saturation of the sample heating power supply until the pyrometer is within a few percent of the set point. Without overshooting, the ribbon temperature is increased 700 K in 21 ms: an average heating rate of 3.3×10^4 K/s. The

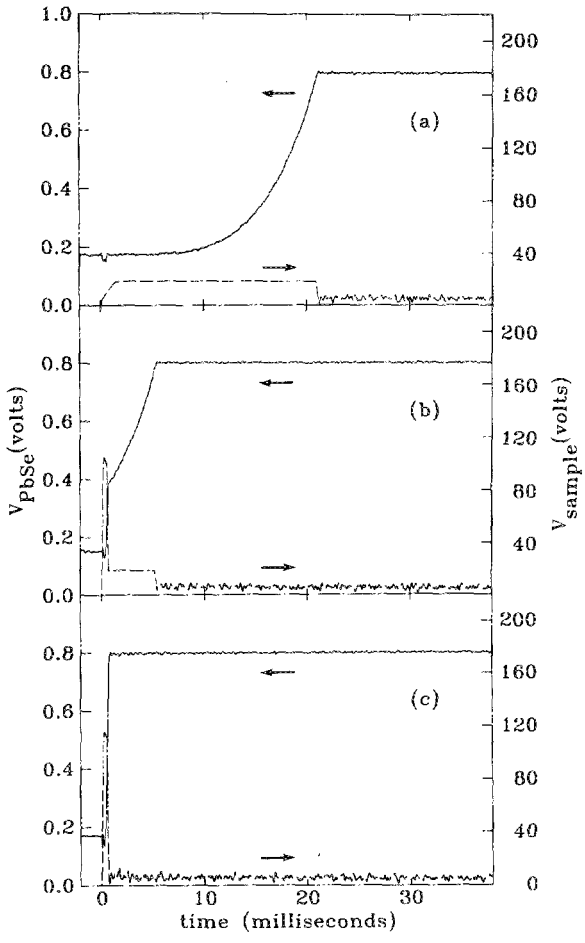

FIG. 7. Time dependence of PbSe pyrometer output (—, left axis) and sample voltage (- - -, right axis) for steps from room temperature to 1000 K. In each step, the set-point temperature is reached without overshoot, and is controlled to $\pm$ 1 K. In (a) the temperature rise time is 21 ms, limited by the saturation of the power amplifier. For (b) and (c), a 500-μs long high-voltage pulse provides several kilowatts of heating power, greatly reducing the time to reach the set-point temperature. The heating rate of (c) is 1.4×10^6 K/s.

small high-frequency fluctuations are due to pyrometer noise. At the temperature shown, the root-mean-square temperature fluctuations are less than 1 K. Using the commercial pyrometer as an independent measure with 10-ms integration, temperature fluctuations of less than 1 K are observed at temperatures as low as 650 K.

It is clear that the loop time response is not applicable to steps of decreasing temperature since power to the sample can at most be shut off. The feedback is then saturated and the system cools with the thermal time constant of the ribbon, τ_t. The available cooling also limits the controllability of rapid first-order phase transitions where a large latent heat must be rapidly dissipated from the sample. Although the current can be turned off by the controller in $\sim 75\ \mu$s, if the sample self-heating power is greater than the available cooling power, temperature control will be lost. Furthermore, we have observed during subsecond crystallization that any inhomogeneity that causes preferential local heating will accelerate the kinetics locally. Without adequate cooling, the latent heat released leads to a further temperature increase and to explosive propagation of the transformation front. Forced convective heat transfer, thinner ribbons, and deposited thin-film samples are being developed to extend our ability to study fast kinetics in these systems.

V. PULSE HEATING

In Fig. 7(a) the rise time for the 700-K step is limited by the saturation of the sample heating supply at 200 W. However, the feedback loop would be capable of controlling the step with a characteristic rise time near $\tau\sim 75\ \mu$s if a fast power amplifier capable of supplying several kilowatts into a few ohms was used. Since this large power is only required during the short temperature rise, a more elegant and economical solution is provided by pulse heating.

Orders of magnitude improvement in heating rate are possible when our power supply is augmented by a 1.5-mF capacitor bank which is charged to ~ 120 V and switched across the sample for the first 500 μs of the step. Instantaneous heating power of over 4 kW is then possible for a 3-Ω specimen. As shown in Fig. 3, the switching is done by a Hexfet transistor,[12] a high-power MOSFET, with a turn-off time of 225 ns. The pulse energy is adjusted by trial and error to that required to bring the sample within a few degrees of the set point. Thereafter, the overdamped controller takes over. Figures 7(b) and 7(c) show the PbSe pyrometer reading and the voltage across the sample during pulse-assisted temperature steps. The exponential decay of voltage on the capacitor bank is visible at the top of voltage each pulse. The heating rate for the 700 K step of Fig. 7(c) is 1.4×10^6 K/s, with nonovershooting control to $\pm$ 1 K. Although other groups have applied constant high current to heat small metallic samples at 10^9 K/s,[13,14] and amorphous metal ribbons at 4×10^4 K/s,[15] this is the first report of controlled temperature steps with heating rates up to one million degrees per second.

Even higher controlled heating rates could in principle be obtained with higher voltage, shorter duration pulses. However, a practical limitation in heating rate without overshoot is determined by the repeatability of heat capacity between samples. Faster rise times would be possible if the power transistor was controlled by the feedback error signal to automatically terminate the pulse at the optimal time.

ACKNOWLEDGMENTS

This research was supported by the Natural Sciences and Engineering Research Council of Canada and les Fonds pour la Formation des Chercheurs et l'Aide á la Recherche de la Province du Québec.

[1] M. Sutton, Y. S. Yang, J. Mainville, J. L. Jordan-Sweet, K. F. Ludwig, Jr., and G. B. Stephenson, Phys. Rev. Lett. **62**, 288 (1989).
[2] K. F. Ludwig, Jr., G. B. Stephenson, J. L. Jordan-Sweet, J. Mainville, Y. S. Yang, and M. Sutton, Phys. Rev. Lett. **61**, 1859 (1988).
[3] M. Sutton, Y. S. Yang, J. Mainville, J. O. Ström-Olsen, Z. Altounian, G. B. Stephenson, and K. F. Ludwig, Jr., Mater. Sci. Eng. **97**, 307 (1988).

[4]S. E. Nagler, R. F. Shannon, C. R. Harkless, M. A. Singh, and R. M. Nicklow, Phys. Rev. Lett. **61**, 718 (1988).
[5]G. B. Stephenson, Nucl. Instrum. Methods Phys. Res. A **266**, 447 (1988).
[6]G. B. Stephenson, K. F. Ludwig, Jr., J. L. Jordan-Sweet, S. Brauer, J. Mainville, Y. S. Yang, and M. Sutton, Rev. Sci. Instrum. **60**, 1537 (1989).
[7]InfraRed Associates, Inc., Cranbury, NJ 08512.
[8]L. N. Neustroev, K. É. Onarkulov, and V. V. Osipov, Sov. Phys. Semicond. **21**, 1352 (1987).
[9]MR-6015-06C, IRCON Inc., Niles, IL 60648.
[10]U. Köster and U. Herold, "Crystallization of Metallic Glasses," in *Glassy Metals I*, edited by H.-J. Güntherodt and H. Beck (Springer, New York, 1981), Chap. 10.
[11]J. Van de Vegte, *Feedback Control Systems* (Prentice Hall, Englewood Cliffs, New Jersey, 1986).
[12]2N6766, International Rectifier, Markham L3R 3L1, Canada.
[13]A. Cezairliyan, High Temp. High Press. **1**, 517 (1969).
[14]A. Cezairliyan, High Temp. High Press. **11**, 9 (1979).
[15]B. Hopstadius and G. Bäckström, Int. J. Thermophys. **4**, 235 (1983).